Annals of Botany **00**: 1–10, 2025
https://doi.org/10.1093/aob/mcaf215, available online at www.academic.oup.com/aob

ANNALS OF BOTANY
Nonprofit since 1887

ORIGINAL ARTICLE

Towards the automatized identification of moss species from their spore morphology

Alix Milis[1,2,*†], Martin Hofmann[3,†], Patrick Mäder[3,4,5,*], Jana Wäldchen[6], Myriam de Haan[2], Petra Ballings[2], Iris Van der Beeten[2], Bernard Goffinet[7] and Alain Vanderpoorten[1,2]

[1]Institute of Botany, University of Liège, B22 Sart-Tilman, Liège B-4000, Belgium, [2]Research and Collection Departments, Botanic Garden Meise, Nieuwelaan 38, Meise B-1860, Belgium, [3]Fakultät für Informatik und Automatisierung, Data-Intensive Systems and Visualization, Technische Universität Ilmenau, Ehrenbergstraße 29, Ilmenau 98693, Germany, [4]German Centre for Integrative Biodiversity Research, iDiv (Halle-Jena-Leipzig), Puschstraße 4, Leipzig 04103, Germany, [5]Faculty of Biological Sciences, Friedrich Schiller University Jena, Fürstengraben 1, Jena 07743, Germany, [6]Department of Biogeochemical Integration, Max Planck Institute for Biogeochemistry, Hans Knöll Strasse 10, Jena 07745, Germany and [7]Department of Ecology and Evolutionary Biology, University of Connecticut, 75 North Eagleville Road, Unit 3043, Storrs, CT 06269-3043, USA
[†]These authors contributed equally to this work.
[*]For correspondence. E-mail ABraipson@uliege.be or Patrick.maeder@tu-ilmenau.de

Received: 17 February 2025 Returned for revision: 08 August 2025 Accepted: 08 September 2025

• **Background and Aims** Automatized species identification tools have massively facilitated plant identification. In mosses, spore ultrastructure appears to be a promising taxonomic character, but has been largely underexploited. Here, we test artificial intelligence-based approaches to identify species from their spore morphology. In particular, we determine whether the number of spores, their polarity, and variation among populations and capsules affect model accuracy.
• **Methods** Scanning electron microscopy spore images were generated for five capsules of five populations in ten species. Convolutional neural networks with a highly modularized architecture (ResNeXt) were trained to identify the species, population and capsule of origin of a spore. The training set was progressively sub-sampled to test the impact of sample size on model accuracy. To assess whether variation in spore morphology among populations affected model accuracy, one population was successively removed to test a model trained on the four remaining populations.
• **Key Results** Species were correctly identified at average rates of 92 %, regardless of polarity. Model accuracy decreased progressively with decreasing sample size, dropping to about 80 % with 15 % of the initial dataset. The population and capsule of origin of a spore was retrieved at rates >75 %, indicating the presence of diagnostic population and capsule markers on the sporoderm. Strong population structure in some species caused a substantial drop of model accuracy when model training and testing was performed on different populations.
• **Conclusions** Spore morphology appears to be an extremely promising tool for moss species identification and may usefully complement the suite of morphological characters used so far in moss taxonomy. The presence of spore diagnostic features at the population and capsule level raises substantial questions on the origin of this structure, which are discussed. Substantial infraspecific variation makes it necessary, however, to train an automatized identification tool from a range of populations and capsules.

Key words: Bryophytes, convolutional neural networks, scanning electron microscopy, species identification, spores, sporoderm, ultrastructure.

INTRODUCTION

Mosses, the most diversified phylum of bryophytes composed of about 13 000 species (Goffinet *et al*., 2008), disperse primarily by spores. The small size of the latter, typically of 10–30 µm, is inversely proportional to their settling velocity (Zanatta *et al*., 2016), which is one of the key parameters of the dispersal capacity of particles in the air (Katul *et al*., 2005). Spores and pollen are thus important components of the atmospheric microbiome (Fröhlich-Nowoisky *et al*., 2016), with up to 100 spores per m^3 in ambient air (Ščevková *et al*., 2024). Not all spores, however, are shaped for wind dispersal. Some exhibit larger sizes than average (e.g. *Archidium*, 150–200 µm) or higher settling velocities than expected given their size (e.g. *Encalypta*

vulgaris) (Zanatta *et al*., 2016), as if dispersal capacity would be counter-selected for in the context of a safe-site strategy (Medina and Estébanez, 2014). As for seeds (Matlack, 1987) and pollen grains (Niklas, 1985), departures of spore settling velocities from expectations based on their size could be caused by variations in their surface ornamentation patterns (Medina and Estébanez, 2014; Zanatta *et al*., 2016).

The ornamentation of the perine, the external-most layer of the spore, was initially described by using light microscopy, leading to the publication of an 'atlas' of European moss spores (Boros, 1975) and the description of morphological groups based on shape and wall structure (Brubaker *et al*., 1998; Passarella and Luizi-Ponzo, 2019). Scanning electron microscopy (SEM) additionally revealed another order of ornamentation above that seen with light microscopy, highlighting striking differences among spores that appear identical under light microscopy (Clarke, 1979).

Spore ultrastructure thus appears as an extremely promising source of taxonomic characters. Clarke (1979) highlighted that spore morphology is most useful at and above the genus level. Smith (1974), for instance, proposed a generic rearrangement of Polytrichaceae supported by spore morphology. Spore morphology has also been used as a key character in identification floras in a few genera, such as *Microbryum* and *Ephemerum* (e.g. Smith, 2004). However, the taxonomic potential of bryophyte spores remains largely under-exploited. As Dickson (1986) noted, no keys exist for the identification of moss spores in palaeoecological studies, challenging their use for reconstructing palaeovegetation, and hence palaeoclimates. In the air biome (Lacey and West, 2006), bryophyte spores are tentatively identified by visual comparison with published photographs such as those of Boros (1975). The only way to achieve certain identification is by growing spores and use available keys for fully developed plants (Barbé *et al*., 2016).

Describing spore morphology and comparing spores is challenging for two reasons. First, spores may be isopolar, with an almost completely spherical shape and a more or less uniform ornamentation pattern (Horton, 1982), or asymmetrical. Spore asymmetry raises the issue of which side is observed, and hence of homologous comparisons among spores. The aperture, a wall specialization located at the proximal pole through which the germ tube emerges (Mogensen, 1983), could at first sight readily serve as a means to unambiguously locate the proximal side. In mosses, four types of aperture can be recognized (Boros, 1975): atreme (without a distinct aperture), katalept (thin-walled trema-like area), trilete (with a triradiate mark that corresponds to the scar left by the union of the proximal sides of the spores in the tetrad) and monolete (with a single straight tetrad scar). A trilete mark is an obvious feature, but is only present in *Sphagnum*, *Takakia* and *Oedipodium* (Renzaglia *et al*., 1997; Brown *et al*., 2015), and typically lacking in the Bryidae ('true' mosses) (Cao and Vitt, 1986; Goffinet *et al*., 2008; Brown *et al*., 2015, but see Boros, 1975; Brubaker *et al*., 1998; and Aslan *et al*., 2022 for reports of a trilete mark in extant Bryidae). The aperture is not distinct in the so-called 'atreme' type (Boros, 1975), which is typically found in pleurocarpous mosses (Boros, 1975; Kungu *et al*., 2007; Alfayate *et al*., 2013), i.e. about half of the moss species diversity. Even in spores described as 'katalept', such as those of *Grimmia* (Boros, 1975), no local specialization, which could be interpreted as an aperture, was observed by Estébanez *et al*. (1997) using SEM and transmission electron microscopy (TEM).

The ornamentation of the perine (the spore outermost layer), which typically varies between the proximal and distal side of the spore, could offer another means to define the polarity of a spore. The distal side of the spore is in contact with the internal capsule tissue called tapetum, which leaves a distinct imprint on the perine, whose external elements are characterized by irregular protuberances and verrucae, and often ornamented by secondary processes (Medina and Estébanez, 2014). The proximal side is in contact with the other spores of the tetrads and is therefore less conspicuously ornamented (Mogensen, 1983). Determining spore polarity from its ornamentation patterns is, however, complicated as the perine elements, made of sporophytic tissues or their remains, may come off, leaving the surface free of verrucae (Medina and Estébanez, 2014). Spore polarity may be unambiguously defined by cytoplasmic features, but the observation of the latter requires TEM imagery (Estébanez *et al*., 1997).

Second, spore morphology may exhibit infraspecific variation, either within or among capsules. Within a capsule, spore size typically follows a unimodal distribution (isospory), but in various cases different categories of spores with different size ranges may be found. For instance, in dioicous species with extreme sexual dimorphism (dwarf males), small (male) and large (female) spores are produced within a single tetrad (anisospory) (Mogensen, 1983). Infraspecific variation has also been reported among capsules in terms of size, but also sporoderm ornamentation (Ireland, 1987). In some species, such as *Lewinskya affine*, infraspecific heterogeneity is higher than interspecific variation (Medina *et al*., 2009). Estébanez *et al*. (1997) therefore concluded that interpopulational variability, especially in geographically remote specimens, could decrease the usefulness of spore ultrastructure as a species-specific marker.

In this context, image-based automated species identification systems appear promising. Initiated about 15 years ago to allow species identification from pictures by non-specialists, such approaches, boosted by the fast-growing availability of plant and animal pictures and substantial progress in machine learning algorithms, notably convolutional neural networks (CNNs), have recently become a reliable alternative to manual identifications (Wäldchen *et al*., 2018, Wäldchen and Mäder, 2018). In plants, identification tools such as Leafnet (Barré *et al*., 2017), Pl@ntNet (https://plantnet.org/) and Flora Incognita (Mäder *et al*., 2021) are now massively used for species identification from photographs by a large public. Artificial intelligence (AI)-based approaches have also increasingly been used for automatized identification of species or higher-level taxa from photographs of pollen grains (Punyasena *et al*., 2022; Matavulj *et al*., 2023) and microscopic algae (Kloster *et al*., 2020; Gunduz and Gunal, 2024; Kwon *et al*., 2025) under light microscopy or SEM.

The present paper aims to investigate whether moss species can, and under what conditions, be identified from the automatized analysis of their spore ornamentation patterns. More precisely, we attempt to address the following questions:

(i) Can CNNs correctly assign a species name from a spore microphotograph, and with what accuracy (Q1)?
(ii) Does spore polarity affect model accuracy (Q2)? Pictures of the distal side, which is often more ornamented than the proximal side, are expected to be more informative for species identification.

(iii) How many pictures are needed to train the network, and how does model accuracy vary depending on the number of spores employed (Q3)?
(iv) To what extent do spores among populations and among capsules within populations vary (Q4a), and how does this affect the sampling design required to efficiently train the network (Q4b)?

MATERIAL AND METHODS

Species selection and specimen sampling

Ten species of Bryophytina *sensu* Goffinet *et al.* (2009) (i.e. peristomate mosses, excluding Takakiophytina, Sphagnophytina, Andreaeophytina and Andreaeobryophytina) were selected to span the range of spore diameter, i.e. from around 8 µm to >200 µm, across the Polytrichopsida (*Polytrichum piliferum* Hedw.) and the Bryopsida. Within the latter, Funariidae [*Encalypta vulgaris* Hedw. and *Physcomitrium pyriforme* (Hedw.) Bruch & Schimp], Dicranidae [*Archidium alternifolium* (Hedw.) Mitt., *Microbryum davallianum* (Sm.) R.H.Zander], Bryidae: Bryales [*Pohlia nutans* (Hedw.) Lindb.], Bartramiales [*Philonotis fontana* (Hedw.) Brid.], Orthotrichales [*Ulota bruchii* (Hornsch. ex Brid.)] and pleurocarps [*Neckeropsis disticha* (Hedw.) Kindb., *Sematophyllum subsimplex* (Hedw.) Mitt.] were sampled. For each species, five capsules from each of five collections were sampled. The collections were selected to maximize geographical distance among populations across species distribution ranges. For species with *trans*-oceanic distributions, such as *Neckeropsis disticha* and *Pohlia nutans*, we sampled collections from the Neotropics and sub-Saharan Africa, and from Europe and North America, respectively. To ensure that fully mature spores were sampled, we focused on capsules that were either already opened but with spores inside, or still operculated but, in species where it is present, with a fully developed peristome, indicative of capsule being mature. A list of the specimens used for the experiments is provided in Supplementary Data Table S1.

Scanning electron microscopy

To minimize distortion or collapse in the vacuum chamber of the scanning electron microscope, spores were dried in a critical-point drier (Anderson, 1951). Prior to critical-point drying, isolated spores were placed on filter paper (medium filtration rate; particle retention >5 µm; VWR International, Leuven, Belgium), which was placed in a sample holder (stainless steel tube with meshed top and bottom, Leica Microsystems Belgium BV, Diegem, Belgium). The latter was submerged for 30 min in 25 % ammonia, 2 × 20 min in 70 % ethanol, 2 × 30 min in dimethoxymethane and left overnight, then 4 × 15 min in acetone. After completion of these preliminary steps, the spores were dried in a critical-point dryer (Leica EP CDP 300, Leica Microsystems Belgium BV) and then mounted on a double-sided carbon sticker (Agar Carbon Tabs, Agar Scientific, Rotherham, UK) taped on a 12.7-mm aluminium specimen stub (Agar Scientific). The stubs were placed in a high resolution fine sputter coater for field emission SEM (JFC-2300HR Coating Unit, JEOL Europe BV, Zaventem, Belgium) and coated with a layer of approximately 6 nm Pt/Pd (using argon-gas, under 0.05 mbar pressure). SEM was carried out with a JEOL JSM-7100FLV field emission SEM (JEOL Europe BV) with a low tension of 1 kV to avoid charging and damaging the samples and a working distance of 6 mm. Magnification ranged from 2000× to 9000× depending on spore size.

Within each capsule, our initial goal was to select five spores for each of the distal, proximal and equatorial views. Defining spore polarity proved, as mentioned above, extremely challenging. As Estébanez *et al.* (1997, 2006) and Medina & Estébanez (2014) previously noted in *Grimmia*, *Ptychomitrium* and *Orthotrichum*, no evident aperture was observed. Polarity was readily defined in some species, such as *Encalypta vulgaris*, whose spores are strongly asymmetric in terms of shape and ornamentation (Fig. 1A). In others, such as in *Polytrichum piliferum*, spores were spherical and hardly displayed variation in ornamentation patterns (Fig. 1B).

Two datasets were generated. Dataset 1 was our 'best' dataset. It included only images of distal views of five spores per capsule in the case of the species for which polarity could be defined (i.e. *Archidium alternifolium*, *Encalypta vulgaris*, *Philonotis fontana*, *Pohlia nutans*, *Polytrichum piliferum*, *Sematophyllum subsimplex* and *Physcomitrium pyriforme*), and an identical number of pictures (125) for the remaining species, for which polarity could not be unambiguously defined. Dataset 2 included additional images of spores in equatorial and proximal view for *Archidium alternifolium*, *Encalypta vulgaris*, *Philonotis fontana*, *Pohlia nutans*, *Polytrichum piliferum*, *Sematophyllum subsimplex* and *Physcomitrium pyriforme*. Because the proximal side tends to be flatter than the distal one, the majority of the spores appear in distal view, so the number of available pictures in equatorial and proximal views differed substantially among species, for a total of 1548 pictures in Dataset 2 (Supplementary Data Table S1).

Data analysis

CNNs were implemented to develop an automatized identification tool of moss species from SEM photographs of their spores. An overview of the workflow is presented in Fig. 2. We used the default parameters of a Python program adapted from an established training protocol (PyTorch Reference Classification, TorchVision maintainers and contributors, 2016) with a ResNeXt-50-32x4d architecture (Xie *et al.*, 2017) and cosine annealing to adaptively adjust the learning rate. The data were split into a training set (80 % of the data) and a test set (20 % of the data). The training phase, during which species names ('class labels') were associated with each training picture, allowed the network to learn spore characteristics ('feature vectors'), establishing a classification rule in a supervised manner. This training process was repeated for 100 epochs (an epoch being one complete pass through all the training images during the learning process), where all training pictures were presented to the network in randomly chosen mini batches per epoch. The iterative training allows the network to optimize the extraction of feature vectors, informing a predictive model that maximizes the link between the predicted species name ('predicted class') and the actual one. Visual inspection of the accuracy vs epoch graph (Supplementary Data Figs S1–S3) confirmed that 100 epochs were sufficient for the model to reach stationarity in terms of accuracy. The model was then used to predict the taxonomic identity of the spores included in the test set, resulting in a confusion matrix reporting the proportion of correctly identified spores, and in the case of misclassified spores, the species to which they were wrongly assigned. We repeated this process 100 times, each time calibrating the model on

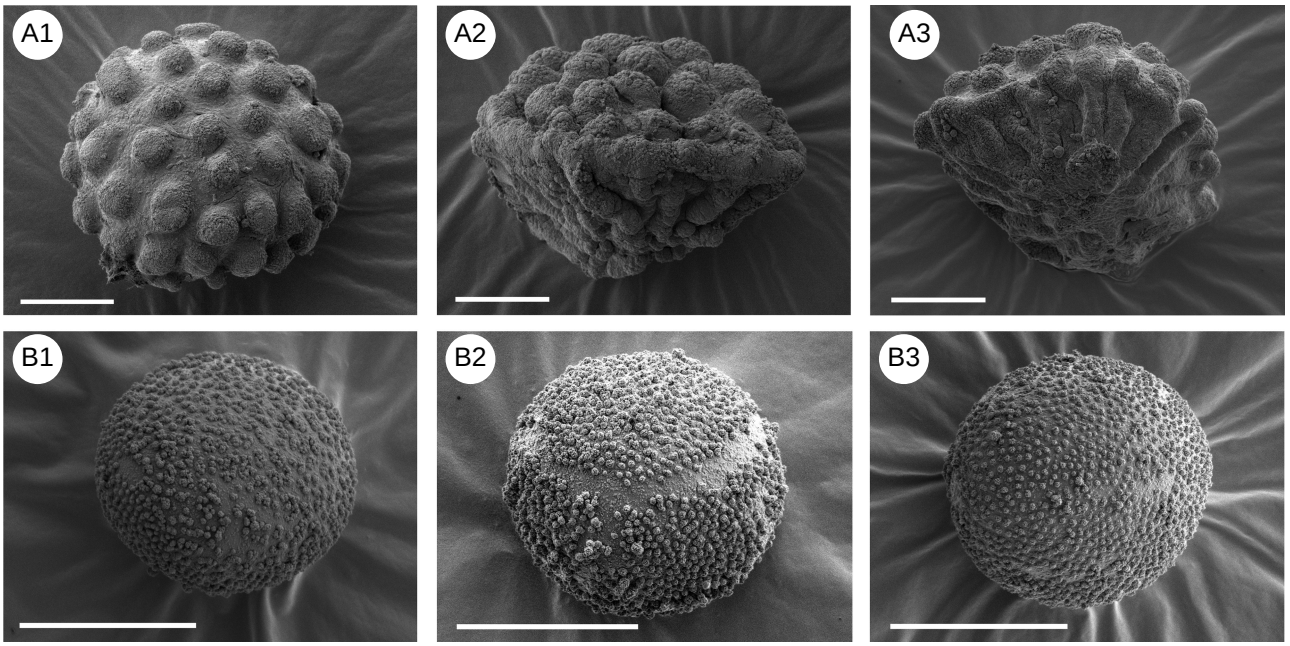

FIG. 1. Selected SEM photographs of the spores of *Encalypta vulgaris* (A) and *Neckeropsis disticha* (B) in distal (1), equatorial (2) and proximal (3) view. In *N. disticha*, polarity could not be defined.

a random sample of 80 % of the data and assessing model accuracy using the 20 % of remaining data (Monte Carlo cross-validation), and reported average model accuracy and its standard deviation across replicates.

One issue with the implementation of such an AI-based approach is that it is unknown what its classification rules actually are. This makes it necessary to develop means to visualize which features of a picture are most relevant to assign the picture to the correct class (here moss species, population and capsule), both to determine which features are actually relevant, but also to make sure that the model does not rely on artefactual information, and in particular background features (Berganzo-Besga *et al.*, 2025, and references therein). To visualize the location of the diagnostic features of the sporoderm used by the CNNs to generate their predictions, a gradient-weighted class activation map, i.e. a heat map highlighting important regions of an image in terms of relevant feature vectors, was generated. The gradient-weighted class activation maps were generated following a procedure named Grad-CAM (Selvaraju *et al.*, 2017). This procedure computes the partial derivatives of a specific class score y^c (e.g. the predicted class c) with respect to the activations A^k of a convolutional layer, and averages them spatially to obtain importance weights $a_k^c = \frac{1}{Z}\Sigma_i\Sigma_j \partial y^c / \partial A_{ij}^k$. The class activation map is then $L^c_{\text{Grad-CAM}} = \text{ReLU}(\Sigma_k\, a_k^c A^k)$, highlighting regions in the input that positively influence the score of class c.

This process was implemented using Dataset 1 and Dataset 2 successively to estimate the effect of integrating spore polarity on model accuracy (Q1–Q2). To determine whether model accuracy depended on the number of spores used during the training phase (Q3), the dataset was subsampled at rates of 90 %, 80 %, …, 15 %. The subsampling was repeated 25 times and, for each replicate, the procedure described above was repeated to determine the proportion of correct classification rate. To assess the extent to which spores vary among populations and among capsules (Q4a), we determined whether there were population or capsule-species markers that allowed the model to correctly identify the population or capsule of origin of a spore. To this end, we subsampled the data in a systematic way within each of the 50 populations and 250 capsules. Thus, at the population level 80 % of the pictures within each population were kept for model training and the remaining 20 % were used for model testing to determine the extent to which the model was able to assign a spore to the correct species and population. The same procedure was implemented at the capsule level. Finally, to determine whether this infraspecific variation among populations and capsules affected the sampling design required to efficiently train the network (Q4b), we successively removed one out of the five populations per species to test the model trained based on the data of the four remaining populations.

RESULTS

When all photographs were used, regardless of polarity, the CNN was able to correctly assign spore SEM photographs to a species at an average rate of 92 ± 6.5 % across the 100 replicates, with a minimum and maximum average rate in *S. subsimplex* (71 ± 10 %) and *E. vulgaris* (100 %), respectively (Table 1a; Supplementary Data Fig. S1). The standard deviation of model accuracy across replicates remained <10 %. Average accuracy did not increase (92 ± 6.5 %) when only distal views for polar spores and any view for apolar ones were employed. In fact, CNNs were able to retrieve the relevant portion of the spore exhibiting diagnostic features. In the case of spores of *E. vulgaris*, which are strongly asymmetrical, informative features were located on both the distal and proximal sides (Fig. 3).

Model accuracy decreased progressively when an increasingly smaller proportion of the data was used to train the model (Supplementary Data Fig. S2), dropping to about 80 % when

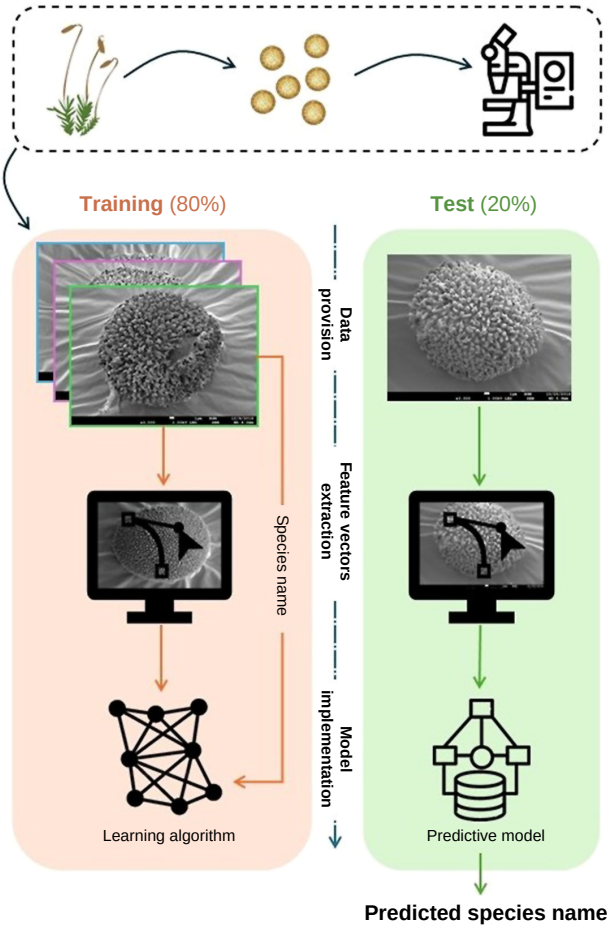

FIG. 2. Overview of the workflow for automatized species identification of mosses from spore photographs under SEM. Spores are sampled from herbarium specimens and are processed under SEM. Neural network training (based on 80 % of the data) and testing (based on the remaining 20 %) is conceptualized graphically in three main steps: data provision, feature vector extraction and model implementation.

only 15 % of the initial dataset was employed in the training phase. CNNs correctly retrieved the population and capsule of origin of a spore with an average accuracy of 75 ± 2 and 77 ± 1 % across species, respectively (Fig. S3), pointing to the existence of phenotypic differences among populations and, within the latter, among capsules (Fig. 4). Finally, when data from an entire population were removed to test a model calibrated on the data from the remaining populations within each species (Table 1b), model accuracy still was on average 75 ± 27 %. There was, however, a substantial variation of model accuracy, but also of the variation of model accuracy among replicates depending on the species. In *Ulota bruchii*, *Encalypta vulgaris* and *Physcomitrium pyriforme*, models trained on four out of five populations and tested on the left-over population had the same accuracy, constant among replicates, as models trained and tested on the entire dataset. In other species, such as *Microbryum davallianum* or *Sematophyllum subsimplex*, model accuracy dropped substantially from 92 and 94 % to 54 and 57 %, respectively, when the model attempted to predict the identity of spores from a population that was excluded from the model calibration. This drop of accuracy was paralleled by a substantial increase of the variation of model accuracy among replicates, with a standard deviation of model accuracy peaking at 41 % in *Archidium alternifolium*.

TABLE 1. Accuracy of an automatized species identification system based on SEM photographs of spores of ten moss species after optimization of the feature vectors in 100 replicates of (a) 80/20 splitting of the entire data into training and test sets, and (b) systematically training the model on four out of the five sampled populations per species and evaluating it based on the remaining population.

Species	Accuracy (a) (%)	Accuracy (b) (%)
Archidium alternifolium	83 ± 6	67 ± 41
Encalypta vulgaris	100 ± 0	97 ± 5
Microbryum davallianum	92 ± 6	55 ± 33
Neckeropsis disticha	86 ± 10	71 ± 8
Philonotis fontana	97 ± 2	80 ± 14
Physcomitrium pyriforme	98 ± 1	87 ± 11
Pohlia nutans	91 ± 5	80 ± 22
Polytrichum piliferum	97 ± 3	61 ± 31
Sematophyllum subsimplex	71 ± 10	57 ± 37
Ulota bruchii	99 ± 1	96 ± 7

The values represent the average ± SD across 100 replicates.

DISCUSSION

The developed CNNs assign moss spores of a sample of ten unrelated species to the correct species with an accuracy of >90 % based on SEM photographs. Such a level of accuracy is similar to that of CNN-based approaches using photomicrographs in other lineages. For instance, 68 diatom species out of a sample of 3027 images were successfully sorted-out out at an accuracy >90 % (Gunduz and Gunal, 2024). In pollen, accuracy levels of between 70 and 97 % were reported among 3–134 pollen types at a taxonomic resolution ranging from species to families (see Punyasena *et al.*, 2022, and references therein). This suggests that CNNs are an extremely promising tool for automatized species identification of moss species based on SEM spore pictures. The relatively high rates of accuracy reported above were achieved from SEM images of spores despite the variability of their sharpness and backgrounds due to, for example, the presence of remains of capsule walls or filter paper used for spore sampling. The method thus seems to be robust to variations in picture quality and be applicable under a range of experimental conditions.

Factors affecting model accuracy

Our results indicate that the ability of the model to assign a spore to the correct species is not affected by the polarity of the spore. In fact, adding spore pictures on the equatorial or proximal view did not lead to a decrease in model accuracy. This may seem paradoxal since, in polar spores, the distal side is typically much more ornamented than the proximal one (Clarke, 1979). Although CNNs do not allow for the characterization of the ornamentation patterns of the spore surface,

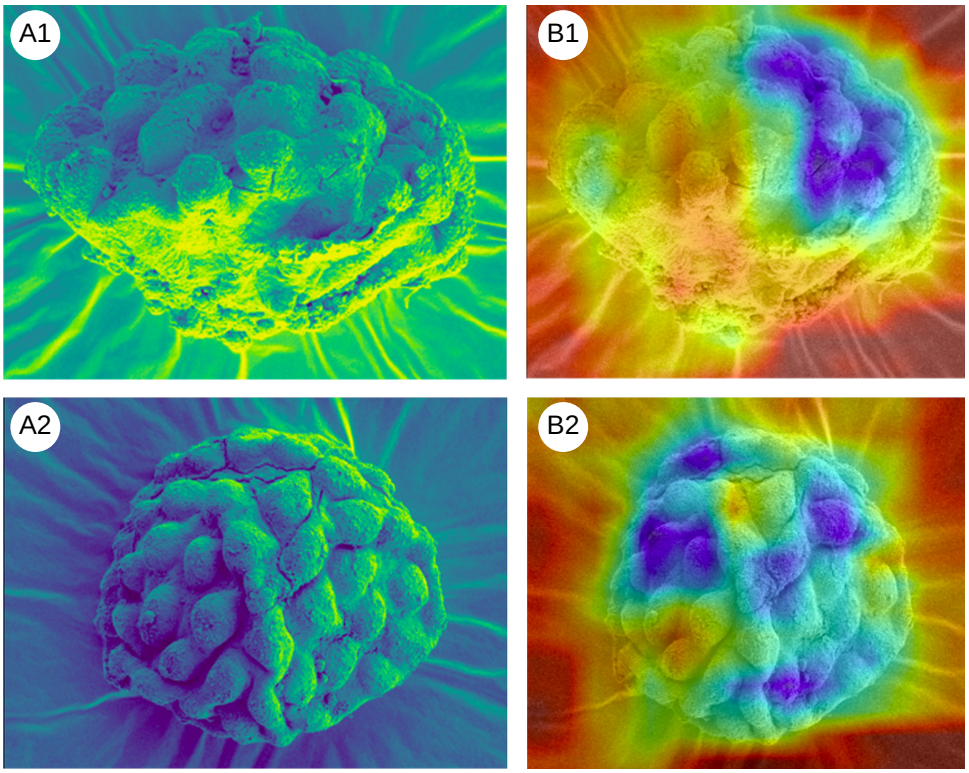

FIG. 3. Initial contrasted SEM pictures (A1, A2) and gradient-weighted class activation maps (B1, B2) of spores of *Encalypta vulgaris* in side (A1, B1) and distal (A2, B2) view, highlighting important regions (in blue) in terms of species-specific features derived by convolutional neural networks.

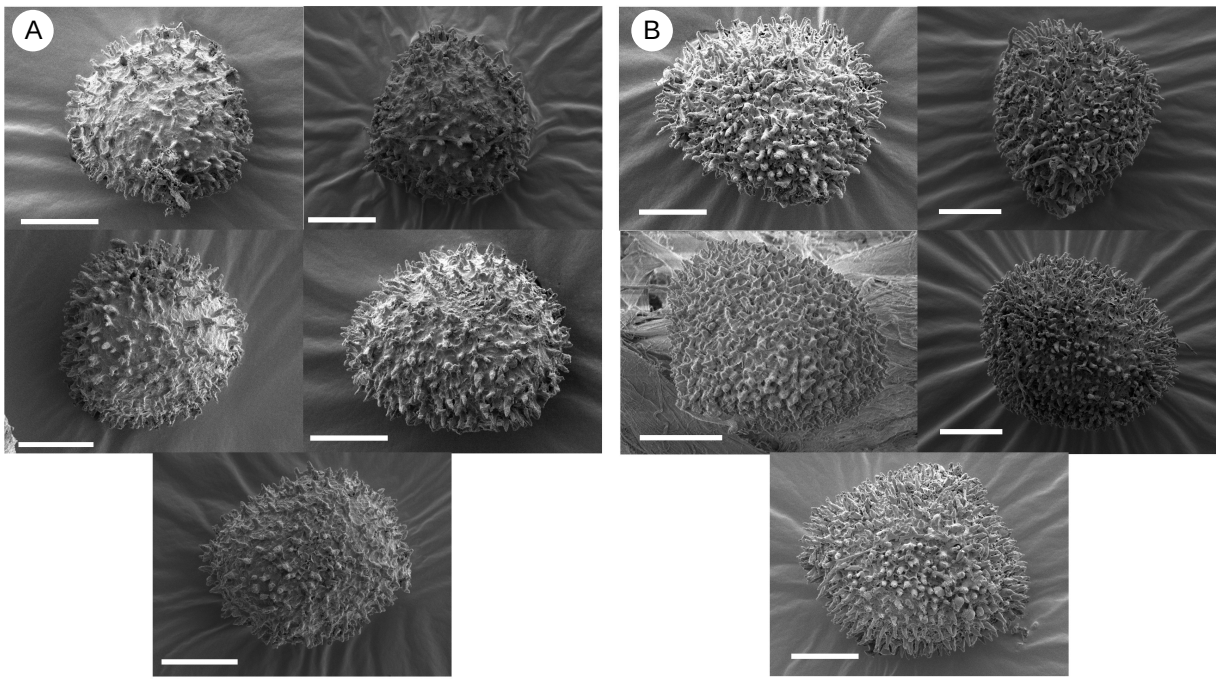

FIG. 4. SEM photographs of spores from two populations (A, B) of *Microbryum davallianum*. White bar represents 10 µm.

gradient-weighted class activation maps highlight the most relevant regions of the spore in terms of diagnostic characters. In the present analyses, these regions were located on both the proximal and the distal side of the spore. CNNs therefore appear to be able to capture specific ornamentation patterns, regardless of spore exposure. It is also possible that, even for photographs of the proximal side, a portion of the side of the spore that holds diagnostic features is most often visible. This is of tremendous

importance because correctly assigning the polarity of the spore, which can prove extremely challenging in the absence of information on the internal structure of the spore by TEM (Estébanez *et al.*, 1997), becomes a non-issue.

Model accuracy varied depending on the number of spores employed to calibrate it. CNNs typically require a large number of observations to avoid overfitting (Goodfellow *et al.*, 2018). Accuracy decreased progressively from >90 % to about 80 % when the training set was reduced to 15 % of the initial set. Based on this, we recommend that, to develop an automatized species identification tool from moss spore SEM photographs of moss spores, about 100 spores per species should be targeted.

Most importantly, the leave-one-out population cross-validation procedure led, in some species, to a substantial drop in model accuracy and a substantial increase of the variation of the latter among replicates, highlighting poor model transferability among populations. In fact, with an accuracy that varied among species, CNNs were able to identify the population and capsule of origin of a spore at average rates >75 %, revealing significant differences in spore morphology among populations and capsules, each characterized by diagnostic markers on the sporoderm. In practice, this suggests that such variation must be used to train the model in order to allow spores from a range of populations and capsules to be correctly assigned to the species.

Intraspecific variation of spore ornamentation

The phenotypic variation of the sporoderm reported here among populations and capsules raises the question of its origin. Spore sampling was restricted here to either open capsules still bearing spores inside, or to fully mature capsules (as indicated by the spreading of a fully developed peristome after lid removal), ruling out differences caused by different ontogenetic stages. Among populations, we suggest that phenotypic differentiation mirrors genetic differentiation due to the random long-distance dispersal of spores and subsequent strong founding effects. In fact, the spore dispersal kernel is typically leptokurtic (Sundberg, 2005). Spore density is maximum around the close vicinity of the mother sporophyte but decreases sharply as a function of the distance from the latter before becoming completely distance-independent after a few hundred metres (Lönnell *et al.*, 2012). This means that once airborne, the vast majority of the spores disperse across very long distances of several hundreds or thousands of kilometres (Sundberg, 2013) before being randomly deposited. This results in a severe founding effect, expressed by high inbreeding coefficient (F_{is}) values within populations (Eppley *et al.*, 2007) and low but significant fixation index (F_{st}) values among populations (see Patiño and Vanderpoorten, 2018 for a review). It is tempting to see in the significant morphological differences between island and continental populations of moss species (Patiño *et al.*, 2014) a signature of such a founding effect.

Several factors may account for the substantial differentiation among spores from different capsules within the same population. In monoicous species, which represent about one-third of moss species (Patiño and Vanderpoorten, 2018), high levels of intragametophytic selfing (within individuals or among individuals from the same spore after clonal fragmentation of the protonema), which generates fully homozygous sporophytes, have been reported (Eppley *et al.*, 2007; Hutsemékers *et al.*, 2013). In dioicous species, by contrast, intergametophytic selfing (among individuals from different spores within the same sporophyte) rarely occurs (Eppley *et al.*, 2007). In fact, one-third of the patches of *Climacium americanum* (Meagher and Shaw, 1990) and two-thirds in *Hylocomium splendens* (Cronberg *et al.*, 1997) include a mixture of genotypes. Whether such a genotypic differentiation translates into differences in spore ornamentation patterns would need to be investigated. Furthermore, it has traditionally been assumed, because the gametophyte is physically attached to the substrate and permanently exposed to environmental variation, that sporophytic features are less plastic than gametophytic ones and, hence, were given primacy in moss classification (Vitt, 1984). The extent to which spore morphology exhibits plastic variation would also need to be further investigated.

Taxonomic applications

The large intraspecific variation of spore ornamentation patterns reported here may usefully complement the suite of morphological characters used so far in moss taxonomy. In mosses, and bryophytes in general, plant body and organ architectures are rather simple and characterized by rampant homoplasy. Bryophyte classification has therefore been substantially challenged by molecular phylogenetics (Bechteler *et al.*, 2023) and molecular characters increasingly provide useful 'barcodes' for species identification (see Dhyani *et al.*, 2024, for a review). In particular, morphologically 'cryptic' species have been increasingly resolved on molecular bases (Kiebacher and Szövényi, 2024, Mikulášková *et al.*, 2024, Nieto-Lugilde *et al.*, 2024, and references therein). Whether spore morphology may contribute to the diagnosis of such species or higher-level taxa characterized primarily on molecular grounds remains to be tested. The preliminary results reported here provide, however, some insights to this question. In fact, the CNN's ability to correctly identify species from spores of a population that was not used for model training was poorest in *Microbryum davallianum* and *Sematophyllum subsimplex*. The former is quite variable morphologically and includes several varieties (Pilkington, 2022), which may well correspond to distinct species. The latter is a widespread Neotropical moss, which, as with other widespread pleurocarpous mosses (e.g. *Hypnum cupressiforme*, Kučera *et al.*, 2019), may well correspond to a complex of species with different sporoderm features. Increasing the accuracy of moss species identification models from their spores thus requires taxonomic improvements. In this regard, spore morphology itself may provide additional taxonomic characters to those of gametophyte and capsule morphology, as exemplified in the genus *Ephemerum*, wherein spore morphology was crucial to diagnose a series of newly segregated species (Holyoak, 2010).

Limitations and further developments

The preliminary results reported here were obtained based on a sample of ten unrelated species. Whether accurate species identification from spore morphology will be achievable in all genera, or whether spore morphology yields, depending on lineages, diagnostic features at genus level or above, as is the case with pollen grains (Punyasena *et al.*, 2022), remains to be tested

by extensive taxon sampling. Previous SEM investigations of moss spores among congeneric species, however, consistently revealed taxonomically informative characters in the sporoderm. In *Ptychomitrium* (Estébanez *et al*., 2006), *Grimmia* (Estébanez *et al*., 1997), *Orthotrichum* (Medina and Estébanez, 2014), *Ulota* (Wang and Jia, 2012), *Pterygoneurum* (Carrión *et al*., 1995) and *Encalypta* (Horton, 1982), species, or species groups, can be diagnosed based on spore ornamentation patterns.

Furthermore, the analyses presented here relied solely on the ornamentation pattern of the sporoderm. Other spore features, and in particular spore size, provide diagnostic characteristics among species in several genera (e.g. *Bryum*, Smith, 2004). Although exhibiting infraspecific variation, especially within the 20 % of moss species that harbour polyploid populations (Patel *et al*., 2019), as is known from ferns (e.g. Dyer *et al*., 2013), potentially blurring interspecific variation, spore size could be integrated to improve the models.

However, adding taxa in the analyses raises a potential concern, that is, whether the model eventually collapses with large species numbers due to homoplasy. As a comparison, AI-based approaches in pollen grains are currently limited to 130 species at most (Punyasena *et al*., 2022).

The approach proposed here also depends strongly on the availability of spore samples. In mosses, sporophyte frequency depends on sexual condition due to the severe constraint that sperm cells need to swim to the archegonia through a continuous film of water. A survey in the UK revealed that 87 % of the species, for which sporophytes are unknown, are dioicous, whereas sporophytes are regarded as occasional to common in 83 % of the monoicous species (Longton, 1997). Thus, developing tools to identify diagnostic spore traits, and hence use such traits to assign spores to species, may be challenging for dioicous species, which represent about two-thirds of moss diversity, due to the scarcity of their sporophytes.

Finally, unlike pollen grains, which can be sorted-out under light microscopy, spore morphology is best revealed under SEM. SEM involves a time-consuming process of spore processing, drying, coating and mounting, and picture acquisition. Thus, unlike online applications, which make vascular plant species identifications using smartphone technologies possible virtually anywhere by a large public (Truong and Van der Wal, 2024), the identification of moss species from their spore morphology will be restricted to much more specific applications by specialists having access to SEM facilities.

CONCLUSION

The present work evidences the usefulness of CNNs as a tool for the standardized identification of moss species from SEM pictures of their spores. This method does not make it necessary to define spore polarity as the ability of the model to distinguish the spores from different species was not affected by the orientation of the spore. The existence of population- and capsule-specific features highlights the necessity of training such a system with a balanced sampling of spores from different capsules and populations. It raises a series of questions about the heritability and plasticity of spore ornamentation patterns. The perspectives to develop an automatized moss species identification tool from spore morphology do not imply the demise of traditional taxonomic approaches because the challenges to find specimens with mature capsules in the wild, combined with the necessity to take SEM photographs of spores, would not make such a tool comparable to plant identification systems such as PlantNet or Flora Incognita based on basic photographs of any part of the plant. Instead, spore morphology offers a suite of characters that have so far been largely underexploited in moss taxonomy and may prove relevant to diagnose species and higher-level taxa currently mostly resolved in a molecular context.

FUNDING

A.M. and A.V. are funded by the Funds for Scientific Research (FRS-FNRS).

ACKNOWLEDGEMENTS

Many thanks are due to a referee for constructive comments on the manuscript.

SUPPLEMENTARY DATA

Supplementary data are available at *Annals of Botany* online and consist of the following. Figure S1. Accuracy of CNNs trained to identify moss species from SEM photographs of their spores after 100 epochs, wherein all training pictures were presented to the network in randomly chosen mini batches per epoch. The lines represent the average accuracy across 100 replicates of 80/20 splitting of the data into training and test sets and the line colour indicates whether all photographs regardless of polarity (all samples) vs only photographs in distal views for polar spores and any view for apparently apolar ones were employed for model training. Figure S2. Accuracy of CNNs trained to identify moss species from SEM photographs of their spores after 100 epochs, wherein all training pictures were presented to the network in randomly chosen mini batches per epoch. The lines and shaded areas represent the average accuracy and its 95 % confidence interval across 100 replicates of 80/20 splitting of the data into training and test sets. Colour indicates the proportion of the initial data that were actually used to train the model while the remaining data were employed for model validation (validation data fraction). Figure S3. Accuracy of CNNs trained to identify the population of origin and, within the latter, the capsule of origin in ten moss species from SEM photographs of their spores after 100 epochs, wherein all training pictures were presented to the network in randomly chosen mini batches per epoch. The lines represent the average accuracy across 100 replicates of 80/20 splitting of the data into training and test sets. Table S1. Numbers of SEM photographs employed to train convolutional neural networks to recognize moss species from their spores depending on the polarity of the latter. Dataset 1 included 125 views in symmetrical spores and 125 distal views (DV) in asymmetrical spores. Dataset 2 included a further sample of available pictures in proximal (PV) and side (SV) views in species with asymmetrical spores.

AUTHOR CONTRIBUTIONS

A.M. and A.V. conceived the project and collected spore samples; M.D.H., P.B. and I.V.D.B. processed and photographed

the spores under SEM; P.M., J.W. and M.H. performed the analyses. A.M., A.V. and B.G. wrote the manuscript, with assistance from all co-authors.

CONFLICTS OF INTEREST

None declared.

DATA AVAILABILITY

The datasets generated and analysed during the current study are available in the FigShare repository, https://doi.org/10.6084/m9.figshare.27620847.v2.

REFERENCES

Alfayate C, **Ron E**, **Estébanez B**, **Pérez-Batista MÁ. 2013**. Mature spores of four pleurocarpous mosses in the Canary Islands: ultrastructure and early germination stages. *The Bryologist* **116**: 97–112. doi:10.1639/0007-2745-116.2.097

Anderson TF. 1951. Techniques for the preservation of three-dimensional structure in preparing specimens for the electron microscope. *Transactions of the New York Academy of Sciences* **13**: 130–134. doi:10.1111/j.2164-0947.1951.tb01007.x

Aslan Z, **Çulha H**, **Ezer T**, **Doğan C. 2022**. Spore morphologies of some acrocarpous mosses (Bryophyta): taxonomical and ecological significance. *Anatolian Bryology* **8**: 106–113. doi:10.26672/anatolianbryology.1189719

Barbé M, **Fenton NJ**, **Bergeron Y. 2016**. So close and yet so far away: long-distance dispersal events govern bryophyte metacommunity reassembly. *The Journal of Ecology* **104**: 1707–1719. doi:10.1111/1365-2745.12637

Barré P, **Stöver BC**, **Müller KF**, **Steinhage V. 2017**. LeafNet: a computer vision system for automatic plant species identification. *Ecological Informatics* **40**: 50–56. doi:10.1016/j.ecoinf.2017.05.005

Bechteler J, **Peñaloza-Bojacá G**, **Bell D**, ***et al.*** **2023**. Comprehensive phylogenomic time tree of bryophytes reveals deep relationships and uncovers gene incongruences in the last 500 million years of diversification. *American Journal of Botany* **110**: e16249. doi:10.1002/ajb2.16249

Berganzo-Besga I, **Orengo HA**, **Lumbreras F**, **Ramsey MN. 2025**. Deep learning black box and pattern recognition analysis using Guided Grad-CAM for phytolith identification. *Annals of Botany* **136**: 355–366. doi:10.1093/aob/mcaf088

Boros Á. 1975. *An atlas of recent European moss spores*. Budapest: Akadémiai Kiadó.

Brown RC, **Lemmon BE**, **Shimamura M**, **Villarreal JC**, **Renzaglia KS. 2015**. Spores of relictual bryophytes: diverse adaptations to life on land. *Review of Palaeobotany and Palynology* **216**: 1–17. doi:10.1016/j.revpalbo.2015.01.004

Brubaker LB, **Anderson PM**, **Murray BM**, **Koon D. 1998**. A palynological investigation of true-moss (Bryidae) spores: morphology and occurrence in modern and late Quaternary lake sediments of Alaska. *Canadian Journal of Botany: Journal Canadien De Botanique* **76**: 2145–2157. doi:10.1139/b98-192

Cao T, **Vitt D. 1986**. Spore surface structure of *Sphagnum*. *Nova Hedwigia* **43**: 191–220.

Carrión JS, **Cano MJ**, **Guerra J. 1995**. Spore morphology in the moss genus *Pterygoneurum* Jur. (Pottiaceae). *Nova Hedwigia* **61**: 481–496. doi:10.1127/nova.hedwigia/61/1995/481

Clarke GCS. 1979. Spore morphology and bryophyte systematics. In: **Clarke GCS**, **Duckett JG.** eds. *Bryophyte systematics*. London: Academic Press, 231–250.

Cronberg N, **Molau U**, **Sonesson M. 1997**. Genetic variation in the clonal bryophyte *Hylocomium splendens* at hierarchical geographical scales in Scandinavia. *Heredity* **78**: 293–301. doi:10.1038/hdy.1997.44

Dhyani A, **Kasana S**, **Uniyal PL. 2024**. From barcodes to genomes: a new era of molecular exploration in bryophyte research. *Frontiers in Plant Science* **15**: 1500607. doi:10.3389/fpls.2024.1500607

Dickson J. 1986. Bryophyte analysis. In: **Berglund B.** ed. *Handbook of Holocene palaeoecology and palaeohydrology*. Chichester: Wiley, 627–643.

Dyer RJ, **Pellicer J**, **Savolainen V**, **Leitch IJ**, **Schneider H. 2013**. Genome size expansion and the relationship between nuclear DNA content and spore size in the *Asplenium monanthes* fern complex (Aspleniaceae). *BMC Plant Biology* **13**: 219. doi:10.1186/1471-2229-13-219

Eppley SM, **Taylor PJ**, **Jesson LK. 2007**. Self-fertilization in mosses: a comparison of heterozygote deficiency between species with combined versus separate sexes. *Heredity* **98**: 38–44. doi:10.1038/sj.hdy.6800900

Estébanez B, **Alfayate C**, **Ron E. 1997**. Observations on spore ultrastructure in six species of *Grimmia* (Bryopsida). *Grana* **36**: 347–357. doi:10.1080/00173139709362628

Estébanez B, **Yamaguchi T**, **Deguchi H. 2006**. Ultrastructure of the spore in four Japanese species of *Ptychomitrium* Fürnr. (Musci). *Grana* **45**: 61–70. doi:10.1080/00173130600555722

Fröhlich-Nowoisky J, **Kampf CJ**, **Weber B**, ***et al.*** **2016**. Bioaerosols in the Earth system: climate, health, and ecosystem interactions. *Atmospheric Research* **182**: 346–376. doi:10.1016/j.atmosres.2016.07.018

Goffinet B, **Buck WR**, **Shaw AJ. 2008**. Morphology, anatomy, and classification of the Bryophyta. In: **Goffinet B**, **Shaw AJ.** eds. *Bryophyte biology*, 2nd edn. Cambridge: Cambridge University Press, 55–138.

Goffinet B, **Buck WR**, **Shaw AJ. 2009**. Addenda to the classification of mosses. I. Andreaeophytina stat. nov. and Andreaeobryophytina stat. nov. *The Bryologist* **112**: 856–857. doi:10.1639/0007-2745-112.4.856

Goodfellow I, **Bengio Y**, **Courville A. 2018**. Deep learning. *Genetic Programming and Evolvable Machines* **19**: 305–307.

Gunduz H, **Gunal S. 2024**. A lightweight convolutional neural network (CNN) model for diatom classification: DiatomNet. *PeerJ: Computer Science* **10**: e1970. doi:10.7717/peerj-cs.1970

Holyoak DT. 2010. Notes on taxonomy of some European species of *Ephemerum* (Bryopsida: Pottiaceae). *Journal of Bryology* **32**: 122–132. doi:10.1179/037366810X12578498136192

Horton DG. 1982. The evolutionary significance of superficial spore characters in the Bryidae. *Journal of the Hattori Botanical Laboratory* **53**: 99–105.

Hutsemékers V, **Hardy OJ**, **Vanderpoorten A. 2013**. Does water facilitate gene flow in spore-producing plants? Insights from the fine-scale genetic structure of the aquatic moss *Rhynchostegium riparioides* (Brachytheciaceae). *Aquatic Botany* **108**: 1–6. doi:10.1016/j.aquabot.2013.02.001

Ireland R. 1987. Scanning electron microscope study of the spores of the North American species of *Plagiothecium* (Musci). *Memoirs of the New York Botanical Garden* **45**: 95–110.

Katul GG, **Porporato A**, **Nathan R**, ***et al.*** **2005**. Mechanistic analytical models for long-distance seed dispersal by wind. *The American Naturalist* **166**: 368–381. doi:10.1086/432589

Kiebacher T, **Szövényi P. 2024**. Morphological, genetic and ecological divergence in near-cryptic bryophyte species widespread in the Holarctic: the *Dicranum acutifolium* complex (Dicranales) revisited in the Alps. *Journal of Plant Research* **137**: 561–574. doi:10.1007/s10265-024-01534-3

Kloster M, **Langenkämper D**, **Zurowietz M**, **Beszteri B**, **Nattkemper TW. 2020**. Deep learning-based diatom taxonomy on virtual slides. *Scientific Reports* **10**: 14416. doi:10.1038/s41598-020-71165-w

Kučera J, **Kuznetsova OI**, **Manukjanová A**, **Ignatov MS. 2019**. A phylogenetic revision of the genus *Hypnum*: towards completion. *Taxon* **68**: 628–660. doi:10.1002/tax.12095

Kungu E, **Longton RE**, **Bonner L. 2007**. Character reduction and peristome morphology in Entodontaceae: constraints on an information source. In: **Newton A**, **Tangney R.** eds. *Pleurocarpous mosses. Systematics and evolution*. Boca Raton: CRC Press, 247–268.

Kwon DH, **Lee MJ**, **Jeong H**, **Park S**, **Cho KH. 2025**. Multi-modal learning-based algae phyla identification using image and particle modalities. *Water Research* **275**: 123172. doi:10.1016/j.watres.2025.123172

Lacey ME, **West JS. 2006**. *The air spora: a manual for catching and identifying airborne biological particles*. Dordrecht: Springer.

Longton RE. 1997. Reproductive biology and life-history strategies. *Advances in Bryology* **6**: 65–101.

Lönnell N, **Hylander K**, **Jonsson BG**, **Sundberg S. 2012**. The fate of the missing spores—patterns of realized dispersal beyond the closest vicinity of a sporulating moss. *PLoS One* **7**: e41987. doi:10.1371/journal.pone.0041987

Mäder P, **Boho D**, **Rzanny M**, ***et al.*** **2021**. The Flora Incognita app—interactive plant species identification. *Methods in Ecology and Evolution* **12**: 1335–1342. doi:10.1111/2041-210X.13611

Matavulj P, **Panić M**, **Šikoparija B**, **Tešendić D**, **Radovanović M**, **Brdar S. 2023**. Advanced CNN architectures for pollen classification: design and

comprehensive evaluation. *Applied Artificial Intelligence: AAI* **37**: 2157593. doi:10.1080/08839514.2022.2157593

Matlack GR. 1987. Diaspore size, shape, and fall behavior in wind-dispersed plant species. *American Journal of Botany* **74**: 1150–1160. doi:10.2307/2444151

Meagher TR, **Shaw J. 1990**. Clonal structure in the moss, *Climacium americanum* Brid. *Heredity* **64**: 233–238. doi:10.1038/hdy.1990.28

Medina NG, **Estébanez B. 2014**. Does spore ultrastructure mirror different dispersal strategies in mosses? A study of seven Iberian *Orthotrichum* species. *PLoS One* **9**: e112867. doi:10.1371/journal.pone.0112867

Medina NG, **Estébanez B**, **Francisco L**, **Mazimpaka V. 2009**. On the presence of dimorphic spores in *Orthotrichum affine* (Bryopsida, Orthotrichaceae). *Journal of Bryology* **31**: 124–126. doi:10.1179/174328209X415086

Mikulášková E, **Peterka T**, **Šmerda J**, **Hájek M. 2024**. Next-generation sequencing reveals hidden genomic diversity in glacial relicts: a case study of *Meesia triquetra*. *Journal of Systematics and Evolution* **62**: 475–488. doi:10.1111/jse.13005

Mogensen GS. 1983. The spore. In: **Schuster RM.** ed. *New manual of bryology*. Nichinan, Japan: Hattori Botanical Laboratory, 325–342.

Nieto-Lugilde M, **Nieto-Lugilde D**, **Piatkowski B**, ***et al.* 2024**. Ecological differentiation and sympatry of cryptic species in the *Sphagnum magellanicum* complex (Bryophyta). *American Journal of Botany* **111**: e16401. doi:10.1002/ajb2.16401

Niklas KJ. 1985. The aerodynamics of wind pollination. *The Botanical Review* **51**: 328–386. doi:10.1007/BF02861079

Passarella MDA, **Luizi-Ponzo AP. 2019**. Palynology of *Amphidium* Schimp. (Amphidiaceae M. Stech): can spore morphology circumscribe the genus? *Acta Botanica Brasilica* **33**: 135–140. doi:10.1590/0102-33062018abb0328

Patel N, **Fawcett S**, **Sundue M**, **Budke JM. 2019**. Evolution of perine morphology in the Thelypteridaceae. *International Journal of Plant Sciences* **180**: 1016–1035. doi:10.1086/705588

Patiño J, **Vanderpoorten A. 2018**. Bryophyte biogeography. *Critical Reviews in Plant Sciences* **37**: 175–209. doi:10.1080/07352689.2018.1482444

Patiño J, **Carine M**, **Fernández-Palacios JM**, **Otto R**, **Schaefer H**, **Vanderpoorten A. 2014**. The anagenetic world of spore-producing land plants. *New Phytologist* **201**: 305–311. doi:10.1111/nph.12480

Pilkington S. 2022. *Microbryum davallianum* (Sm.) R.H.Zander in Britain and Ireland. *Field Bryology* **127**: 2–7.

Punyasena SW, **Haselhorst DS**, **Kong S**, **Fowlkes CC**, **Moreno JE. 2022**. Automated identification of diverse Neotropical pollen samples using convolutional neural networks. *Methods in Ecology and Evolution* **13**: 2049–2064. doi:10.1111/2041-210X.13917

Renzaglia K, **McFarland K**, **Smith D. 1997**. Anatomy and ultrastructure of the sporophyte of *Takakia ceratophylla* (Bryophyta). *American Journal of Botany* **84**: 1337. doi:10.2307/2446132

Ščevková J, **Štefániková N**, **Dušička J**, **Lafférsová J**, **Zahradníková E. 2024**. Long-term pollen season trends of *Fraxinus* (ash), *Quercus* (oak) and *Ambrosia artemisiifolia* (ragweed) as indicators of anthropogenic climate change impact. *Environmental Science and Pollution Research International* **31**: 43238–43248. doi:10.1007/s11356-024-34027-w

Selvaraju RR, **Cogswell M**, **Das A**, **Vedantam R**, **Parikh D**, **Batra D. 2017**. Grad-CAM: visual explanations from deep networks via gradient-localization. *Proceedings of the IEEE International Conference on Computer Vision (ICCV)*, Venice, Italy, pp. 618–626. doi:10.1109/ICCV.2017.74

Smith AJE. 2004. *The moss flora of Britain and Ireland*. Cambridge: Cambridge University Press.

Smith GL. 1974. New developments in the taxonomy of Polytrichaceae: epiphragm structure and spore morphology as generic characters. *Journal of the Hattori Botanical Laboratory* **38**: 143–150.

Sundberg S. 2005. Larger capsules enhance short-range spore dispersal in *Sphagnum*, but what happens further away? *Oikos* **108**: 115–124. doi:10.1111/j.0030-1299.2005.12916.x

Sundberg S. 2013. Spore rain in relation to regional sources and beyond. *Ecography* **36**: 364–373. doi:10.1111/j.1600-0587.2012.07664.x

TorchVision maintainers and contributors. 2016. TorchVision: PyTorch's computer vision library. *GitHub repository*. https://github.com/pytorch/vision (14 April 2025, Date accessed)

Truong MXA, **Van der Wal R. 2024**. Exploring the landscape of automated species identification apps: development, promise, and user appraisal. *BioScience* **74**: 601–613. doi:10.1093/biosci/biae077

Vitt DH. 1984. Classification of the Bryospida. In: **Schuster RM.** ed. *New manual of bryology*. Nichinan: Hattori Botanical Laboratory, 696–759.

Wäldchen J, **Mäder P. 2018**. Plant species identification using computer vision techniques: a systematic literature review. *Archives of Computational Methods in Engineering: State of the Art Reviews* **25**: 507–543. doi:10.1007/s11831-016-9206-z

Wäldchen J, **Rzanny M**, **Seeland M**, **Mäder P. 2018**. Automated plant species identification—trends and future directions. *PLOS Computational Biology* **14**: e1005993. doi:10.1371/journal.pcbi.1005993

Wang Q-H, **Jia Y. 2012**. A taxonomic revision of the Asian species of *Ulota* Mohr (Orthotrichaceae). *The Bryologist* **115**: 412–443. doi:10.1639/0007-2745-115.3.412

Xie S, **Girshick R**, **Dollár, P**, **Tu Z**, **He K. 2017**. Aggregated residual transformations for deep neural networks. *2017 IEEE Conference on Computer Vision and Pattern Recognition (CVPR)*, Honolulu, HI, USA, pp. 5987–5995, doi:10.1109/CVPR.2017.634

Zanatta F, **Patiño J**, **Lebeau F**, ***et al.* 2016**. Measuring spore settling velocity for an improved assessment of dispersal rates in mosses. *Annals of Botany* **118**: 197–206. doi:10.1093/aob/mcw092